IJCRT.ORG ISSN : 2320-2882

INTERNATIONAL JOURNAL OF CREATIVE RESEARCH THOUGHTS (IJCRT)

An International Open Access, Peer-reviewed, Refereed Journal

Structural And Electrical Properties Of Sn Doped $Ba_{1-X}sn_xfe_{12}o_{19}$ Nanoparticles

[1]Pawan Kumar [2]Pramod kumar Singh [3]B.P.Maurya [4]Sanjay Singh

[1]Department of Physics, Govt. Degree College, Razanagar, Swar, Rampur -244924

[2]Department of Physics, Shri Sadguru Saibaba Science and Commerce College Ashti-442707

[3]Department of Physics Ganjdundwara(PG) College Ganjdundwara,Kasganj-207242

[4]Department of Physics, Chintamani College of Arts and Science Gondpipri-442702

ABSTRACT

Barium ferrites substituted by tin (Sn) with general formula $Ba_{1-x}Sn_xFeO_{19}$ (x=0.0 0.1 0.2 0.3) have been prepared by co precipitation method by using the ammonium solution co percipient agent. The samples were characterized by X-ray (XRD), scanning electron microscopy (SEM). The XRD analysis confirms the hexagonal phase formation for all the compounds and indicates that all Sn ions are situated into the lattice of barium ferrite with extra pick of Fe_2O_3. The crystallite size of all the samples were measured from XRD data. Scanning electron microscopy was carried out to observe the morphology of the synthesized $Ba_{1-x}Sn_xFeO_{19}$ ferrites. Temperature-dependent dc electrical resistivity of Tin doped Barium ferrites was investigated as a function Sn concentration. Here, in present study, the effects of Sn doping consecration on particle size and electrical properties are mainly studied.

Keywords: Barium ferrites, Ferromagnetism, Resistivity

1. INTRODUCTION

The barium hexaferrites ($BaFe_{12}O_{19}$) have been widely studied as potential materials for magnetic recording and microwave absorption [1-7]. For these applications, high saturation magnetization, a suitable coercivity and low temperature coefficients of coercivity and remanence are desired. To obtain good quality of barium ferrite materials, various methods have been used for their preparation and a large number of investigations have been carried out to modify these properties. To develop hexagonal ferrites with enhanced properties for magnetic recording applications, a new chemical substitution was introduced. Barium hexaferrite possesses a hexagonally close-packed lattice composed of oxygen, barium, and iron atoms. Its unit cell structure is represented as SRS*R*, where the asterisk (*) indicates that the block is rotated relative to the c-axis. The S (Fe_6O_8) and S* structural blocks are spinels, each comprising two oxygen layers and six Fe^{3+} ions occupying both octahedral and tetrahedral sites. The R (AFe_6O_{11}) and R* blocks consist of three hexagonally packed oxygen layers, each containing four oxygen ions, with one of these oxygen ions replaced by a barium ion [3]. Kimura et al. first reported multiferroic behavior in a single-phase $Ba_{0.5}Sr_{1.5}Zn_2Fe_{12}O_{22}$ hexaferrite at room temperature [8]. Subsequently, several other research groups also observed multiferroic properties in single-phase hexaferrite materials [9]. Chen et al. reported pronounced ferroelectricity and strong ferromagnetism in barium hexaferrite ceramics [10]. More recently, Ghahfarokhi et al. investigated the magnetic and electric properties of $PbFe_{12}O_{19}$ hexaferrite [11], while Tokunaga et al. examined the magnetic and magnetoelectric characteristics of Sc-substituted $BaFe_{12-x}Sc_xO_{19}$ single crystals [12]. Pawan et al. also observed multiferroic properties in lead-doped barium hexaferrite [13].

Therefore, in present work, we have tried to synthesize Sn-doped M-type barium ferrite $Ba_{1-x}Sn_xFeO_{19}$ (x=0.0 0.1 0.2 0.3) by co-precipitation method. Finally, the structural and temperature-dependent dc electrical resistivity of Ba ferrites has been investigated as a function Sn concentration.

2. MATERIALS AND METHODS

The Sn-doped $Ba_{1-x}Sn_xFeO_{19}$ (x = 0.0, 0.1, 0.2, 0.3) samples were synthesized using the co-precipitation technique. The starting reagents—barium acetate ($Ba(CH_3COO)_2$), ferric nitrate nonahydrate ($Fe(NO_3)_3 \cdot 9H_2O$), tin nitrate ($Sn(NO_3)_4$), citric acid ($C_6H_8O_7$), and ammonia solution—were all of analytical grade and used without further purification. Initially, measured amounts of barium acetate, ferric nitrate, and tin nitrate were dissolved in 50 ml of deionized water under continuous stirring at 60 °C. Citric acid was then added to the resulting Ba^{2+}, Sn^{2+}, and Fe^{3+} solution to form chelated complexes, maintaining a 1:1 molar ratio between citric acid and the total metal ions. The pH was adjusted to 12 by the dropwise addition of ammonia solution, leading to the co-precipitation of a gel-like product. This gel was dried at 100 ℃ for 24 h, then further heated up to 250 ℃ to obtain a dry, brown, loose powder through combustion. The resultant precursor was calcined at 1000 °C for 2 h to achieve the hexagonal phase of $Ba_{1-x}Sn_xFeO_{19}$ (x=0.0, 0.1, 0.2, 0.3). The crystalline phases of the synthesized powders were characterized by X-ray diffraction (Rigaku Mini Flex 200, CuKα radiation, λ = 1.54 Å) within the 2θ range of 20°–80°, using a step size of 0.02°/min. The surface morphology of all samples was analyzed using a scanning electron microscope (SEM). To investigate the DC electrical transport behavior of barium hexaferrite and Sn-substituted barium ferrite, DC resistivity measurements were performed through the four-probe technique with a high-precision Keithley DMM6500 Digital Multimeter (Model DRMSS42).

3. RESULTS AND DISCUSSION

The X-ray diffraction (XRD) patterns of Sn-doped $Ba_{1-x}Sn_xFeO_{19}$ (x = 0.0, 0.1, 0.2, 0.3) powders sintered at 1000 ℃ for 2 hours in air are presented in Fig. 1(b). The XRD results confirm the formation of a single hexagonal phase for all compositions, indicating that Sn ions are successfully incorporated into the barium ferrite lattice, with a minor peak corresponding to Fe_2O_3 and no other impurity phases detected. Structural parameters such as lattice constants (a, c), unit cell volume (V), and average crystallite size were determined from the XRD data and summarized in Table 1. The lattice parameters (a and c) were calculated using the relation corresponding to the (107) and (114) diffraction planes [14].

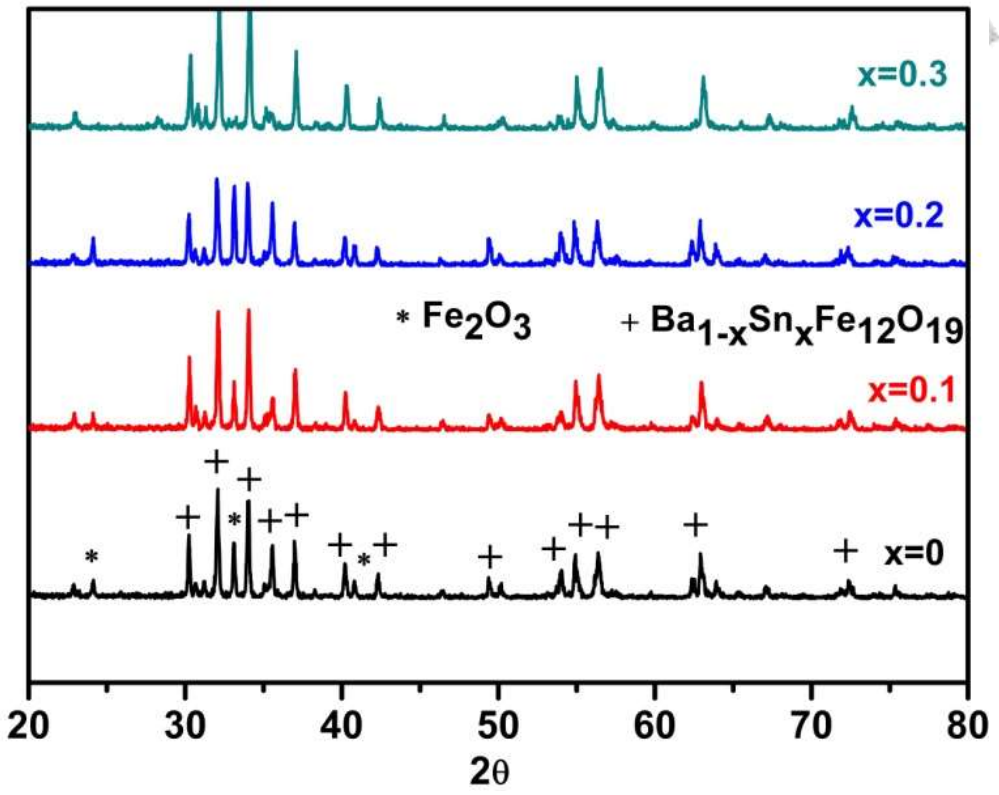

Figure 1: X-Ray diffraction pattern of $Ba_{1-x}Sn_xFe_{12}O_{19}$ (x=0.0, 0.1, 0.2, 0.3) nanoparticles

$$\frac{1}{d^2} = \frac{4}{3}\left(\frac{h^2+hk+k^2}{a^2}\right) + \frac{l^2}{c^2} \quad \text{..... (1)}$$

The unit cell volume has been determine by the formula

$$V = \frac{\sqrt{3}}{2} a^2 c \quad \text{..... (2)}$$

The crystallite size of all the samples was determined using the well-known Debye-Scherrer formula, from the line widths of the strongest diffraction peak.

$$D = \frac{(0.94)\lambda}{\beta_D cos\theta} \quad \text{..... (3)}$$

Where β_D is full width at half maximum (FWHM), K=0.94 is the shape factor, λ is the wavelength of X-rays, and θ is Bragg angle [14].

The obtained value of crystallized size, lattice parameter and cell volume calculated from the above equation for the prepared samples are listed in Table 1. It is revealed from Table 1 that that the crystallite size decrease from ~44.28 nm to ~29.82 nm by increasing doping content from x=0 to 0.4, which can be happened, due to the barium atom has a larger atomic radius compared to a tin atom, so the size of Tin doped barium ferrite unite cell is decreased which results decrease the crystal size [15]. The observed value of lattice parameter: a (5.862 Å – 5.812 Å) and the cell volume (689.99–676.40Å) are similar to the previously reported values [4, 15].

sample	Crystal size	Lattice Parameter		V(Å)^3
		a(Å)	c(Å)	
X=0	44.28nm	5.862	23.186	689.99
X=1	37.69nm	5.844	23.180	685.59
X=2	32.09nm	5.825	23.158	680.49
X=3	29.82nm	5.812	23.122	676.40

Table 1: Variations of crystallite size, Unit Cell Volume, lattice parameters of Sn doped $Ba_{1-x}Sn_xFe_{12}O_{19}$ (x=0.0, 0.1, 0.2, 0.3) nanoparticles

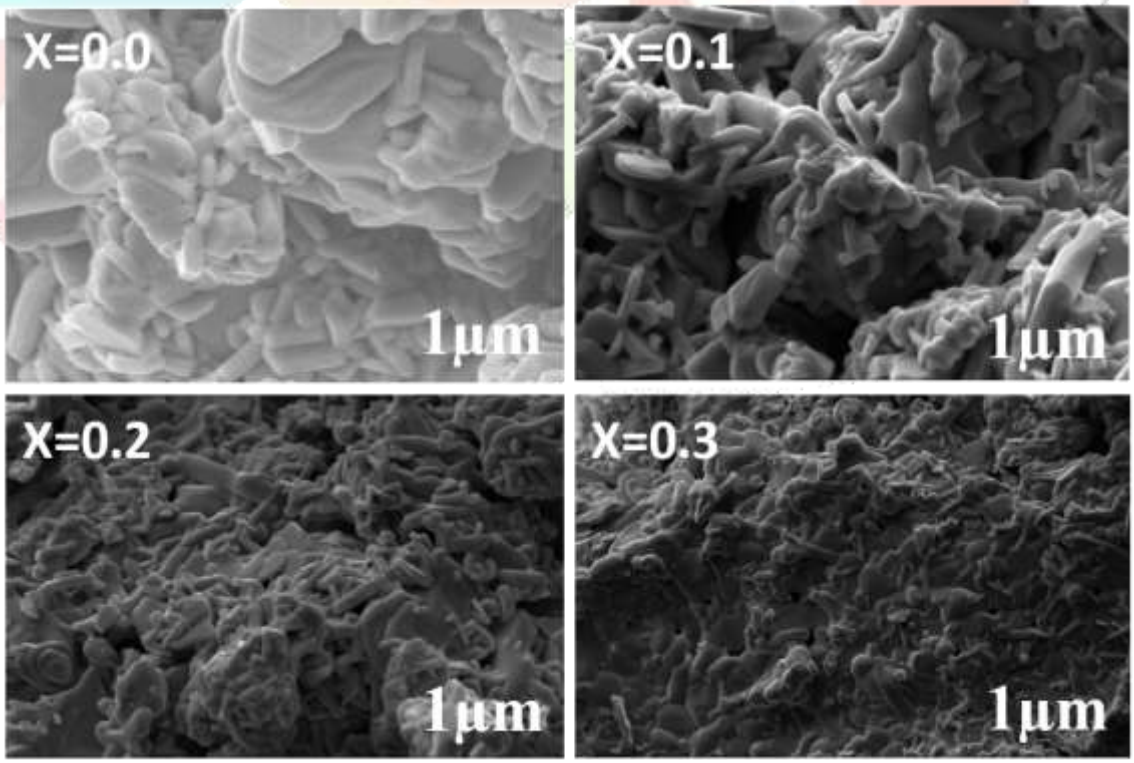

Figure 2: SEM picture for pure and Sn doped $Ba_{1-x}Sn_xFe_{12}O_{19}$ (x=0.0, 0.1, 0.2, 0.3) nanoparticles

Figure 2 displays the scanning electron micrograph images of of $Ba_{1-x}Sn_xFe_{12}O_{19}$ (x=0.0, 0.1, 0.2, 0.3) nanoparticles. The morphology showed that the sample particles had smooth exterior faces. Hexagonal particles that are well linked are arranged nearly identically, further the hexagonal platelet-like grains structure are also observed for all the prepared samples as previously reported [15-18]. The morphology revealed that the ferrite particles were distributed in a nearly homogeneous size. The produced samples have crystallite sizes between 44 and 30 nm.

The measurement of DC resistivity as a function of temperature was conducted for all samples $Ba_{1-x}Sn_xFe_{12}O_{19}$ (x=0.0, 0.1, 0.2, 0.3 within the range of 300 to 573 K, as illustrated in figure 3. The results indicated that the resistivity of the synthesized Sn doped barium ferrite material diminished with rising temperature across all samples, thereby confirming the semiconductor characteristics of the produced materials. Verwey's hopping mechanism elucidates that the variation in charge carrier mobility with increasing temperature is attributed to the hopping of electrons between adjacent Fe^{3+} ions. As the temperature escalated, the probability of hopping increased, leading to enhanced conductivity of the synthesized materials [19]. Further, as increase the content of Sn in barium ferrite, the resistivity of the barium ferrite decrease sharply with temperature. Which indicate increase the conductivity behaviour due to the tin ion H=has two oxidation states +4 and +2 that's increase the charge mobility.

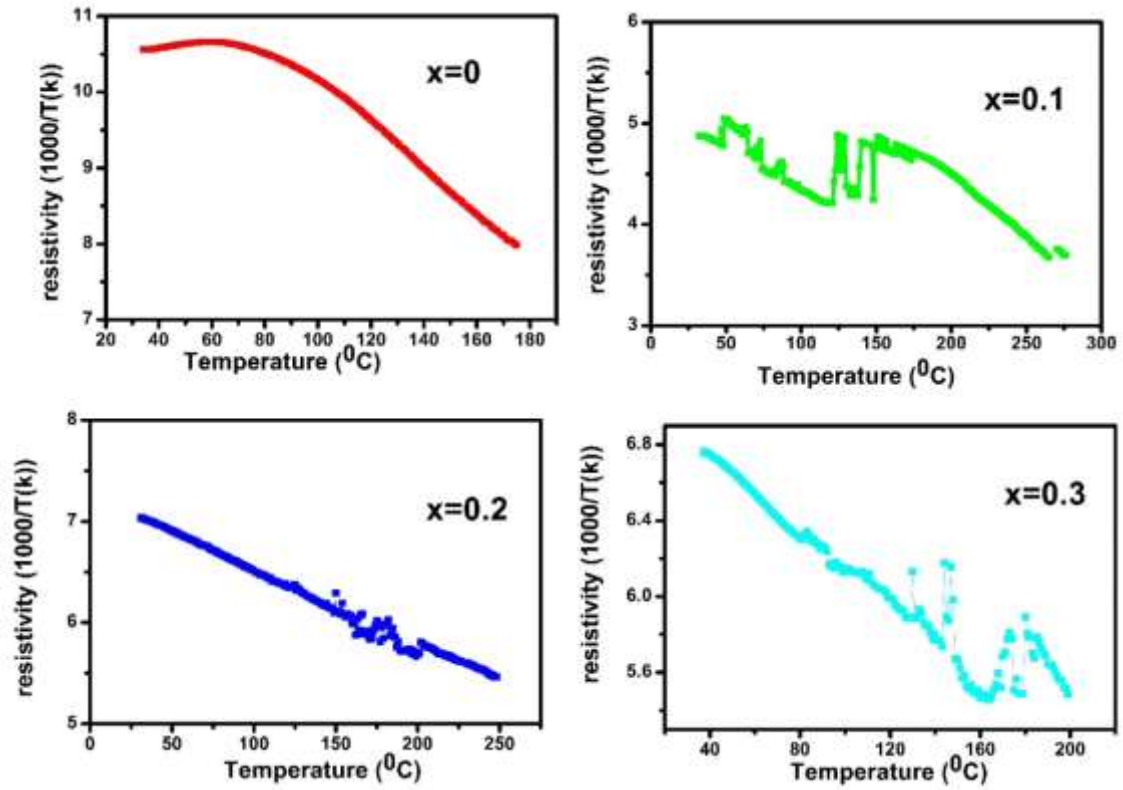

Figure 3: Temperature dependent DC resistivity plot of $Ba_{1-x}Sn_xFe_{12}O_{19}$ (x=0.0, 0.1, 0.2, 0.3)

4. CONCLUSION

In conclusion, Sn-doped $Ba_{1-x}Sn_xFeO_{19}$ (x=0.0 0.1 0.2 0.3) samples has been prepared by co-precipitation method. XRD patterned for all the samples demonstrate confirms the hexagonal phase formation and the crystallite size decrease from ~44.28 nm to ~29.82 nm by increasing doping content from x=0 to 0.4. The SEM results describe the formation of hexagonal platelet-like grains structure. DC resistivity Sn doped barium ferrite material decrease with rising temperature across all samples indicate the semiconductor characteristics was observed for the prepared materials.

ACKNOWLEDGEMENT

Author (PK) is thankful to Department of Physic, NIT, Kurukshetra, for providing all the measurement facilities.

REFERENCES:

[1] R. Valenzuela, Novel applications of ferrites, Phys. Res. Int. 2012 (2012) ID 5918.

[2] V.G. Harris, A. Geiler, Y. Chen, S.D. Yoon, M. Wu, A. Yang, Z. Chen, P. He, P. V. Parimi, X. Zuo, C.E. Patton, M. Abe, O. Acher, C. Vittoria, Recent advances in processing and applications of microwave ferrites, J. Magn. Magn. Mater. 321 (2009) 2035–2047.

[3] R.C. Pullar, Hexagonal ferrites: a review of the synthesis, properties and applications of hexaferrite ceramics, Prog. Mater. Sci. *57*(7) (2012) 1191-1334

[4] Kaczmarek, W. A., Calka, A., & Ninham, B. W. (1992). Preparation of fine, hollow, spherical BaFe12O19 powders. *Materials chemistry and physics*, *32*(1), 43-48.

[5] Ali, I., Islam, M. U., Awan, M. S., & Ahmad, M. (2013). Effects of Ga–Cr substitution on structural and magnetic properties of hexaferrite (BaFe12O19) synthesized by sol–gel auto-combustion route. *Journal of Alloys and Compounds*, *547*, 118-125.

[6] Dong, A., Liu, R., Tian, Z., Peng, F., Zhao, R., Su, X., & Tang, R. (2023). Effect of pre-sintering particle size on the microstructure and magnetic properties of two-step hot-press prepared BaFe12O19 thick films. *Journal of Alloys and Compounds*, 171683.

[7] Akbarsharifi, A., Ashouri, F., Pourashraf, T., & Yousefi, M. (2025). Magnetism and exchange coupling in BaFe12O19/ZnFe2O4 as a hard/soft nanocomposite. *Journal of Solid State Chemistry*, *342*, 125102.

[8] T. Kimura, G. Lawes and A. P. Ramirez, "*Electric polarization rotation in a hexaferrite with long-wavelength magnetic structures"*, PRL, **94** (2005) 137201-4.

[9] A. V. Trukhanov, S. V. Trukhanov, V. G. Kostishin, L. V. Panina,I. S. Kazakevich, V. A.Turchenko, V. V.Kochervinskii, M. M. Salem, and D. A. Krivchenya, "*Multiferroic properties and structural features of M-typeAl-substituted barium hexaferrites",* Physics of the Solid State, **59** (2017) 737–745.

[10] G. Tan, X. Chen, "Structure and multiferroic properties of barium hexaferrite ceramics", J. Magn. Magn.Mater., **327** (2013) 87–90.

[11] Farjadian, F., Abbaspour, S., Sadatlu, M. A. A., Mirkiani, S., Ghasemi, A., Hoseini-Ghahfarokhi, M., ... & Hamblin, M. R. (2020). Recent developments in graphene and graphene oxide: Properties, synthesis, and modifications: A review. *ChemistrySelect*, *5*(33), 10200-10219.

[12] Jiang, X., Jia, H., Wu, C., Yu, Z., Luo, H., Guo, R., ... & Sun, K. (2020). Cation distribution and magnetic characteristics of textured BaFe12-xScxO19 hexaferrites: Experimental and theoretical evaluations. *Journal of Alloys and Compounds*, *835*, 155202.

[13] Kumar, P., Gaur, A., & Kotnala, R. K. (2017). Magneto-electric response in Pb substituted M-type barium-hexaferrite. *Ceramics International*, *43*(1), 1180-1185.

[14] B.D. Cullity, Elements of X-ray diffraction, 2nd edition, Addison-Wesley Publ. Co. Read. MA. (1978) 100-105-279

[15] Topal, U., Ozkan, H., & Dorosinskii, L. (2007). Finding optimal Fe/Ba ratio to obtain single phase BaFe12O19 prepared by ammonium nitrate melt technique. *Journal of alloys and compounds*, *428*(1-2), 17-21.

[16] Topal, U., Ozkan, H., & Sozeri, H. (2004). Synthesis and characterization of nanocrystalline BaFe12O19 obtained at 850 C by using ammonium nitrate melt. *Journal of magnetism and magnetic materials*, *284*, 416-422

[17] Sözeri, H., Küçük, İ. L. K. E. R., & Özkan, H. (2011). Improvement in magnetic properties of La substituted BaFe12O19 particles prepared with an unusually low Fe/Ba molar ratio. *Journal of Magnetism and Magnetic Materials*, *323*(13), 1799-1804.

[18] Yu, J., Tang, S., Zhai, L., Shi, Y., & Du, Y. (2009). Synthesis and magnetic properties of single-crystalline BaFe12O19 nanoparticles. *Physica B:Condensed Matter*, *404*(21), 4253-4256.

[19] Lakshman, A., Rao, P. S., Rao, B. P., & Rao, K. H. (2005). Electrical properties of In3+ and Cr3+ substituted magnesium–manganese ferrites. *Journal of Physics D: Applied Physics*, *38*(5), 673.